International Journal of Civil, Mechanical and Energy Science, 6(6)
Nov-Dec, 2020 | Available: http://ijcmes.com/

Thinning and springback prediction of Mg alloy AZ31 in deep drawing process – Influence of BHF and friction conditions

Marina Maia Araripe[1], Francisco Elicivaldo Lima[2], Rômulo do Nascimento Rodrigues[3]

[1,2]Manufacturing, Quality and Sustainability Center (NMQS), Department of Mechanical engineering, Federal University of Ceará, Brazil
[3]Mechanical Vibration Laboratory (LVM), Department of Mechanical engineering, Federal University of Ceará, Brazil

Abstract*— *Magnesium is nowadays the lighter metal used in structural applications with expressive advantages over steel and aluminum. Due to its low density and high specific strength, magnesium alloys represent a promising alternative, especially for applications in automobile industry, being used in structural components in order to reduce weight and, consequently, improve fuel efficiency. In the recent decades, several researches have been performed in order to improve the use of Mg alloys in forming process since its formability is strongly affected by some conditions as temperature. In this study, a Finite Element Analysis (FEA) is performed to simulate the sheet metal deep drawing process of the magnesium alloy AZ31. The main objective is to evaluate the effect of the blank holder force and friction conditions in the formability by predicting results of springback, thickness distribution and thinning of the sheet metal blank. In total, 54 simulations were performed.

Keywords*— *Blank holder force, Deep drawing, Finite elements, Friction, Lightweight alloy, Metal forming, Springback, Thickness distribution.

I. INTRODUCTION

In the past decades, the use of lightweight structures for several industrial fields, specially vehicles manufacturers, have been progressively encouraged due to decrease of fuel consumption and decline in CO_2emissions into the atmosphere [1]. Among the lightweight metals, magnesium and its alloys has gained much attention due to its density and high strength-to-weight ratio among other structural metals [2]. Besides, magnesium alloys have superior qualities like recycling facility, better manufacturability and good dimensional stability.

Generally, the traditional methods to test metal forming properties are experimentally, applying trial-and-error and empirical-techniques, which are costly and time-consuming, since the whole tooling part, such dies, blank holders and punches needs to be designed and manufactured. By using a finite element model and simulating it, it is possible to predict several results and save resources, as time and money. Numerical simulation not only acts as a design verification tool, but also becomes an important method to explore the optimization of process parameters [3,4,5].

There are many significant forming parameters that are influencing on deep drawing process, such as punch nose radius, die shoulder radius, blank holder force, coefficients of friction, forming temperature, punch speed, clearance between punch and die and others. Among there, blank holder force and coefficients of friction play a vital role in the final quality of the workpiece, being fundamental parameters in order to prevent the appearance of ears, wrinkles and even the failure.

The main objective of this work is to simulate the deep drawing process of magnesium alloy AZ31 and evaluate the effect of blank holder force and friction coefficients in final thickness distribution, thinning of the blank and springback.

54 non-linear simulations were performed: 27 dynamic (deep drawing) and 27 static (springback). The first type lasted 0,028s and the second one, 0,1s.

ISSN: 2455-5304
https://dx.doi.org/10.22161/ijcmes.66.1

II. SIMULATION OF DEEP DRAWING PROCESS

2.1 Finite element model

Fig. 1 shows the model of the tooling. The blank is a circular sheet that will be positioned between the blank holder and the die. Dimensions regarding the die, punch, blank holder and blank are given in Table 1. Due to the symmetry, the numerical analysis of the deep drawing process was performed by using just one quarter of the model in order to fit in the nodes limit permitted by Abaqus Student Version.

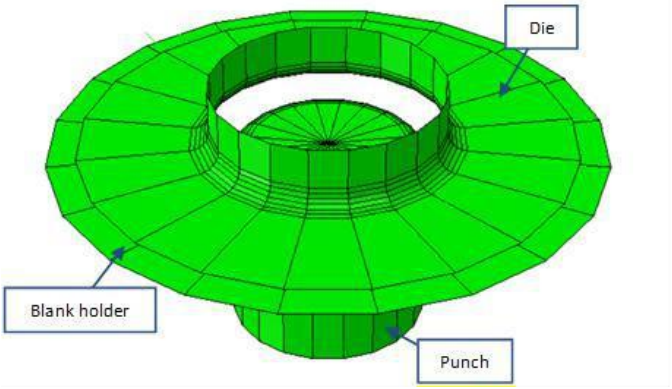

Fig. 1: Model of the drawing tooling

Table 1: Parameters' geometrical dimensions

Sheet	
Radius	50 mm
Thickness	1.2 mm

Punch	
Depth	49mm
Nose radius	5 mm
Radius	25 mm

Die	
Height	15.5 mm
Shoulder radius	5 mm
Min. radius	29.83 mm
Max. Radius	62.8 mm

Blank holder	
Height	1.2 mm
Profile radius	2mm
Min. radius	39.83 mm
Max. Radius	70.18mm

Regarding the meshing, the blank sheet was the only part considered deformable with a planar shell base and it was meshed with S4R shell type element [6], the element size was 2.5. The tooling was modeled by using analytical rigid form. Neither the punch, die and blank holder were meshed.

2.2 Material properties

The blank is made of Mg alloy AZ31. In order to represent the material some properties of the alloy were informed to the software, those are given in Table 2 [7]. Besides, to describe the plastic behavior, the True Stress x True Strain curve were calculated following the parameters in Table 3.

Table 2: Properties of AZ31 alloy

Density	1.77×10^{-9}
Young's Modulus	45000 MPa
Poisson's ratio	0.35

Table 3: Flow stress calculation parameters

Strain hardening exponent	n =	0.18565966
Hardening coefficient	K=	302.913767
Temperature	T(K) =	523
Strain rate	e (s^{-1})	0.1
Strain rate sensitivity exponent	m =	0.09925048

In Table 3, only 2 parameters were chosen: temperature and strain rate. The others were also calculated by using the equations (1-3) [8]:

$$n = 0.031 + 0.013 \log \dot{\varepsilon} + \frac{97.1}{T} \quad (1)$$

$$m = \frac{-145.263}{T} + 0.377 \quad (2)$$

$$K = -156.4 + 9.1 \log \dot{\varepsilon} + \frac{244980.4}{T} \quad (3)$$

The parameters' result calculation is as shown in Table 3. Then were used equations (4,5) to estimate the true stress x true strain curve shown in Fig. 2, which was validated by being compared with others flow stress curves obtained experimentally under the same conditions (temperature and strain rate) [8, 9].

$$\sigma = K\varepsilon^n \dot{\varepsilon}^m \quad (4)$$

$$\sigma = 18015\ \varepsilon 0.16 \dot{\varepsilon} 0.083 \exp(-0.0078T - 0.8903\varepsilon) \quad (5)$$

(4) is valid to deformation values (ε) between 0.02 and 0.3, temperature values (T) between 423 and 573K and strain rate values ($\dot{\varepsilon}$) between 0.1 and 0.0001s^{-1}. While (5) is valid to deformation values (ε) between 0.15 and 0.45, temperature values (T) between 473 and 573K and strain rate values ($\dot{\varepsilon}$) between 0.1 and 0.0001s^{-1}.

ISSN: 2455-5304
https://dx.doi.org/10.22161/ijcmes.66.1

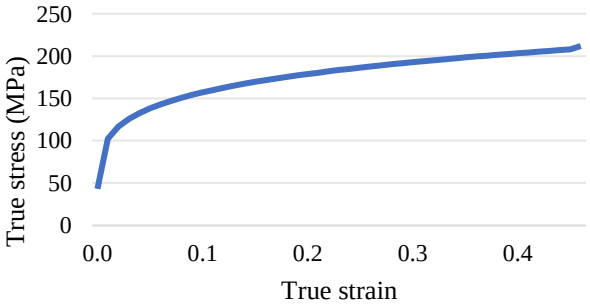

Fig. 2: True stress x true strain of AZ31 alloy (T = 523K and $\dot{\varepsilon}$ = 0.1s-¹)

Furthermore, in order to describe the anisotropic behavior of the Mg alloy, Lankford coefficients obtained experimentally by Reddy [9] were used to evaluate anisotropic parameters according to Hill's criteria (6-8).

$$r_0 = 1.30$$

$$r_{45} = 2.50$$

$$r_{90} = 1.05$$

By assuming $R_{11} = R_{13} = R_{23} = 1$:

$$R_{22} = \sqrt{\frac{r_{90}(r_0+1)}{r_0(r_{90}+1)}} \quad (6)$$

$$R_{33} = \sqrt{\frac{r_{90}(r_0+1)}{(r_0+r_{90})}} \quad (7)$$

$$R_{12} = \sqrt{\frac{3(r_0+1)r_{90}}{(2r_{45}+1)(r_0+r_{90})}} \quad (8)$$

Then resulting as shown in Table 4:

Table 4: Anisotropy parameters of AZ31

Anisotropy parameters AZ31 alloy					
R_{11}	R_{22}	R_{33}	R_{12}	R_{13}	R_{23}
1	0.9519	1.013735	0.716819	1	1

2.3 Drawing operation parameters

2.3.1 Blank holder force (BHF)

The force applied by the blank holder aim to prevent wrinkling and depends on limit drawing ratio (LDR), blank's thickness and blank's material. The BHF required in deep drawing process varies from very little to a maximum of one third of the drawing pressure [10]. The higher the BHF, the greater will be the strain over the punch face, although the drawing process is limited by the strain in the side-wall.

In the present work, a range regarding the blank holder force was considered varying from 0.1 kN to 35 kN.

2.3.2 Lubrication conditions

The friction in deep drawing plays a vital role in deep drawing affecting the stress and strains in the blank during the forming work. Besides, it is one of the major factors that determine the required punch force and blank holder force. Therefore, lubrication conditions affect the energy needed to deform the sheet. Concluding, the optimization of the friction coefficients is an important task in order to obtain an acceptable workpiece shape and to improve the energy efficiency. In the present work, two friction coefficients were considered:

- Friction coefficient between upper surface and punch and blank holder (μ_u): varying from 0.05 to 1.0

- Friction coefficient between lower surface and die ($_l$): varying from 0.05 to 0.5.

2.4 Output extraction

2.4.1 Thickness distribution

The study of thickness distribution is important to rate the uniformity of the blank walls and the behavior of each region of the workpiece. This factor was evaluated by creating a path of 8 nodes along the blank, from the center to the extremity of the blank and extracting the section thickness value of each node.

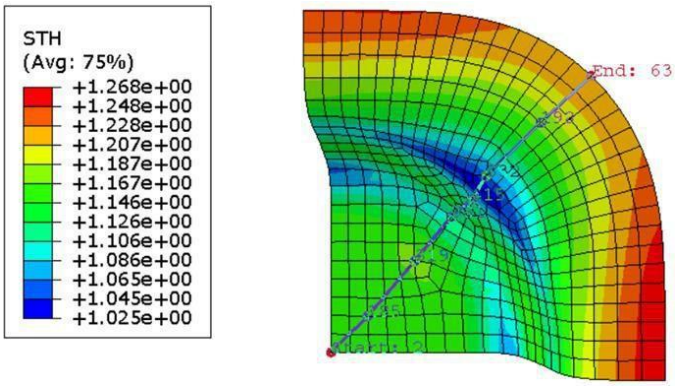

Fig. 3: STH node path along the blank after deep drawing process

Fig. 3 illustrates the thickness variation in each region. Since the initial blank thickness was 1.2 mm, by looking to the scale, is possible to notice that the thickness walls varied from 1.025 to 1.268 mm approximately after deep drawing. Nevertheless, in the present study, the results were not just evaluated by analyzing the scale colors. A report with the exactly STH values of each node was extracted from each simulation.

2.4.2 Thinning

In order to evaluate the thinning of each region, the equation (9) was utilized.

$$STHIN = 1 - \frac{STH}{STH_{orig}} \quad (9)$$

In which,

STHIN = thickness thinning (%);

STH = evaluated thickness (mm);

STH_{orig} = original thickness (mm).

The thinning was evaluated for each node according to the previous item and the average thinning of the nodes was calculated for each simulated condition.

2.4.3 Springback

Alike to thickness distribution evaluation method, a set of nodes was established, but another path was adopted, as illustrated in Fig. 4. In addition, all possible nodes were selected, totaling 22.

To evaluate the springback it was necessary to perform a static explicit non-linear simulation, in which the beginning was characterized by the final results of the previous simulation (deep drawing) and the difference between the two was both in type (this one being static and the previous one, dynamic), as in privation of contact with the other components of the process (blank holder, die and punch).

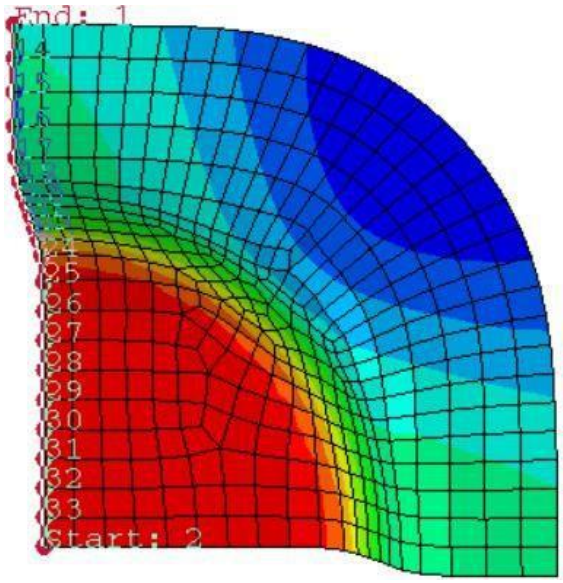

Fig. 4: Springback node path along the blank after deep drawing process

The results used were those of magnitude, also obtained in a report format. The difference between magnitudes obtained at the beginning of the static simulation (end of the dynamic) and at the end of the static simulation (conclusion of the springback) was calculated and the simple average was performed, obtaining the percentage of springback under the referred conditions.

III. RESULTS AND DISCUSSION

3.1 Blank holder effect

3.1.1 In thickness distribution

Analyzing the Table 5, it appears that the average that keep closest to the original thickness of the blank (1.2 mm) is the one obtained with the application of 25 kN load. However, it was observed that with the load of 30 kN the standard deviation was the smallest calculated, being therefore the load that provides less disparity in thickness along the blank. From a different perspective, it appears that the value of 0.1 kN presented both the farthest average from the original thickness and the largest standard deviation.
From Fig. 5, it is clear that for all applied blank holder forces, the most discrepant point from the others is '3', which corresponds to a region close to the bottom fold of the cup. As expected, the regions closest to the center of the glass, at the bottom, '1' and '2' suffered a slight accumulation of material, while the '5 to 8' wall regions suffer a loss due to stretching. The obtained curve is similar to the results of another study [11] regarding the influence of the force of the blank holder on the distribution of final thickness.

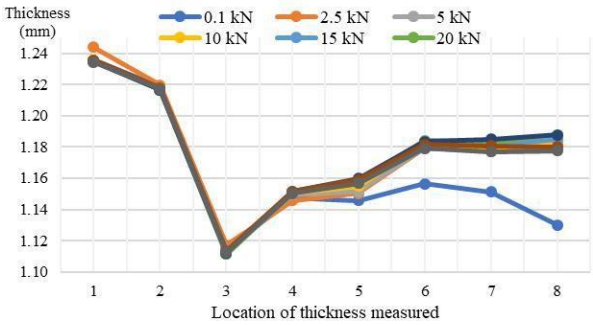

Fig. 5: BHF effect in thickness distribution

Table 5: BHF effect in thickness distribution

Measured Locations (mm)	BHF (kN)								
	0.1	2.5	5	10	15	20	25	30	35
1	1.236	1.244	1.235	1.235	1.235	1.235	1.235	1.236	1.235
2	1.219	1.220	1.217	1.217	1.217	1.217	1.217	1.218	1.217
3	1.115	1.117	1.114	1.113	1.112	1.111	1.112	1.114	1.112
4	1.148	1.146	1.149	1.150	1.151	1.151	1.152	1.152	1.150
5	1.146	1.150	1.152	1.155	1.157	1.158	1.160	1.159	1.157
6	1.157	1.180	1.180	1.182	1.184	1.184	1.184	1.182	1.179
7	1.151	1.177	1.178	1.179	1.181	1.183	1.185	1.181	1.177
8	1.130	1.179	1.180	1.182	1.185	1.188	1.188	1.180	1.178
Average	1.162	1.177	1.176	1.177	1.178	1.178	1.179	1.178	1.176
Standard deviation	0.042	0.041	0.038	0.039	0.039	0.039	0.038	0.038	0.038

3.1.2 In thinning

Table 6: BHF effect in thinning (%)

Measured Locations (mm)	BHF (kN)								
	0.1	2.5	5	10	15	20	25	30	35
1	0.030	0.037	0.030	0.030	0.029	0.029	0.029	0.030	0.029
2	0.016	0.017	0.014	0.014	0.014	0.014	0.014	0.015	0.014
3	0.071	0.069	0.072	0.073	0.074	0.074	0.073	0.072	0.073
4	0.044	0.045	0.042	0.041	0.041	0.041	0.040	0.040	0.041
5	0.045	0.041	0.040	0.037	0.036	0.035	0.033	0.034	0.036
6	0.036	0.017	0.017	0.015	0.013	0.013	0.014	0.015	0.017
7	0.041	0.019	0.018	0.017	0.016	0.014	0.012	0.016	0.019
8	0.058	0.017	0.017	0.015	0.013	0.010	0.010	0.017	0.019
Average	0.043	0.033	0.031	0.030	0.029	0.029	0.028	0.030	0.031
%	4.26	3.27	3.12	3.04	2.94	2.89	2.82	2.99	3.11

From the Table 6. it is possible to notice the significant thinning in the '3' region. as previously observed in the analysis of the thickness distribution.

From Fig. 6 it can be noticed that the greatest thinning occurs with the application of the smallest BFH (0.1 kN) and that there is a downward trend to the minimum (25 kN), from which the thinning grows again. This behavior can be explained by the fact that higher BHF values result in increased tensions in the glass walls [11].

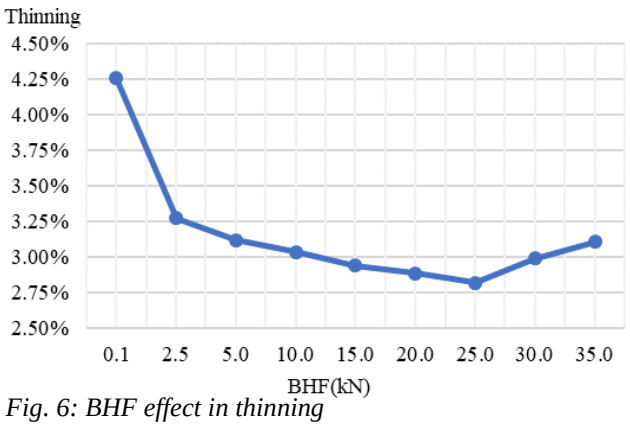

Fig. 6: BHF effect in thinning

ISSN: 2455-5304
https://dx.doi.org/10.22161/ijcmes.66.1

3.1.3 In springback

The blank holder force is one of the parameters of vital influence on the springback. It is a consensus among countless authors that the optimized application of BHF is the solution for high springback values and other problems of deep drawing.

From the Table 7 and the Fig. 7, it is possible to perceive a point of minimum spring back when the BHF applied is 5 kN and a subtle growth trend as the blank holder force increases. This same behavior, in which the springback increases subtly as the BHF increases, was found by other research in which numerous experimental tests were carried out in order to study the influence of BHF on the springback [12].

Table 7: BHF effect in springback (%)

BHF (kN)								
0.1	2.5	5	10	15	20	25	30	35
0.43	0.46	0.35	0.35	0.36	0.36	0.37	0.37	0.38

From the Table 7 and the Fig. 7, it is possible to perceive a point of minimum spring back when the BHF applied is 5 kN and a subtle growth trend as the blank holder force increases. This same behavior, in which the springback increases subtly as the BHF increases, was found by other research in which numerous experimental tests were carried out in order to study the influence of BHF on the springback [12].

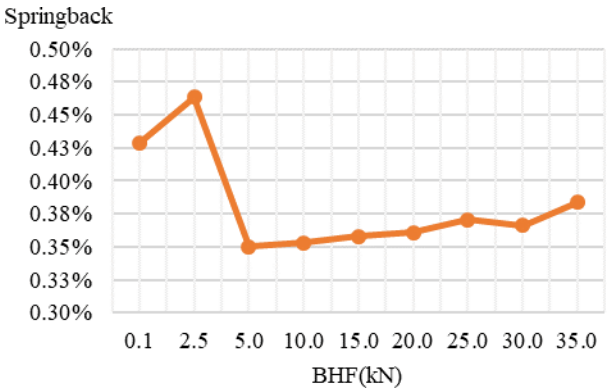

Fig. 7: BHF effect in springback

3.2 Friction coefficient between upper surface, blank holder and punch effect

As previously discussed, friction has a significant effect on the metal conformation. Two factors influence the friction coefficient value: the nature of the surfaces in contact and the nature of the lubricant used. For the present work, friction coefficient ranges were considered according to Mang and Dresel [13].

3.2.1 In thickness distribution

Table 8: Upper friction coefficient effect in thickness distribution

	Fluid lubricant					Solid lubricant				Dry lubricant
Measured Locations (mm)	μ_u									
	0.05	0.1	0.15	0.3	0.5	0.55	0.6	0.65	07	1
1	1.242	1.239	1.235	1.224	1.218	1.217	1.217	1.216	1.215	1.209
2	1.230	1.223	1.216	1.199	1.197	1.197	1.197	1.197	1.197	1.194
3	1.146	1.129	1.111	1.049	1.086	1.113	1.127	1.136	1.144	1.159
4	1.162	1.157	1.151	1.131	1.086	0.980	0.788	0.855	0.829	0.691
5	1.153	1.155	1.157	1.160	1.164	1.164	1.164	1.162	1.161	1.115
6	1.178	1.181	1.184	1.190	1.193	1.194	1.194	1.195	1.195	1.193
7	1.175	1.178	1.181	1.188	1.192	1.192	1.193	1.193	1.193	1.193
8	1.179	1.182	1.185	1.190	1.193	1.193	1.194	1.194	1.194	1.194
Average	1.183	1.180	1.178	1.166	1.166	1.156	1.134	1.143	1.141	1.119
							Failure occurred			

From the simulations' results shown in Table 8 and Fig. 8, the occurrence of failure was found when coefficients of friction applied to the upper surface of the blank are equal to or greater than μ = 0.55, this happens due to the increase in stresses, and consequently deformations. It is also observed that the point where there is a failure is '4', an equivalent region to the bottom edge of the cup.

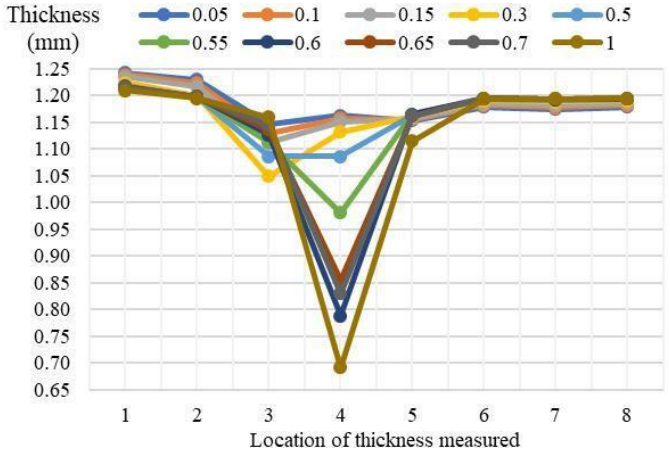

Fig. *8: Upper friction coefficient effect in thickness distribution*

At Fig. 8, there is a significant difference in thickness in the '4' region, starting from μ = 0.60. In addition, it is observed that for μ-values up to 0.15, the thickness distribution is considerably uniform.

3.2.2 In thinning

The results obtained for the thinning shown in Table 9 and Fig. 9 point at two mean peaks, one at μ = 0.6 and the other at μ = 1, this one being considered the value that provides lower uniformity pieces. On the other hand, good uniformity is observed as the friction coefficient decreases, although μ values between 0.05 and 0.5 show very close values. Despite this apparent better uniformity that the lower friction value presents, it is important to consider the formation of wrinkles and ears, which is quite recurrent in friction values that are too low on the upper surface of the blank, especially in the flange region, regarding contact with the blank holder.

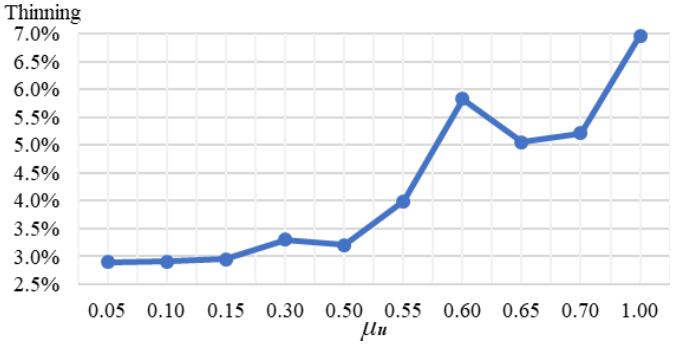

Fig. 9: Upper friction coefficient effect in thinning

Table 9: Upper friction coefficient effect in thinning

	Fluid lubricant				Solid lubricant				Dry lubricant	
Measured Locations (mm)	μ_u									
	0.05	0.1	0.15	0.3	0.5	0.55	0.6	0.65	0.7	1
1	0.035	0.032	0.029	0.020	0.015	0.014	0.014	0.013	0.012	0.008
2	0.025	0.019	0.014	0.001	0.002	0.002	0.002	0.002	0.003	0.005
3	0.045	0.059	0.074	0.126	0.095	0.073	0.061	0.054	0.046	0.034
4	0.031	0.036	0.041	0.057	0.095	0.183	0.343	0.288	0.309	0.424
5	0.039	0.037	0.036	0.033	0.030	0.030	0.030	0.032	0.032	0.071
6	0.018	0.016	0.013	0.009	0.006	0.005	0.005	0.005	0.004	0.006
7	0.021	0.018	0.016	0.010	0.007	0.007	0.006	0.006	0.005	0.006
8	0.018	0.015	0.013	0.008	0.006	0.006	0.005	0.005	0.005	0.005
Average	0.029	0.029	0.029	0.033	0.032	0.040	0.058	0.051	0.052	0.070
%	2.90	2.91	2.94	3.30	3.20	3.99	5.83	5.05	5.22	6.96

ISSN: 2455-5304
https://dx.doi.org/10.22161/ijcmes.66.1

3.2.3 In springback

Table 10: Upper friction coefficient effect in springback (%)

Fluid lubricant				Solid lubricant	Dry lubricant
μ_u					
0.05	0.1	0.15	0.3	0.5	0.5 - 1
0.40	0.38	0.36	0.27	0.22	**Failure occurred**

Not considering the criteria of wrinkling and ear formation, from the results previously shown, it would certainly be concluded that the adequate values for friction of the upper surface would follow the rule of "the smaller, the better". On the other hand, the results obtained for the springback lead to a reconsideration. As explained in the previous item, the thinning averages obtained for μ from 0.05 to 0.5 were very close. As shown in Table 10 and Fig. 10, the springback values are significantly different. For μ = 0.5, a springback of 0.22% was obtained, practically half of the value obtained for μ = 0.05 (0.40%).

Possibly, the ideal value for the upper friction would be between μ = 0.15 and μ = 0.30, to obtain reasonable values for both the elastic return and the uniformity of the part.

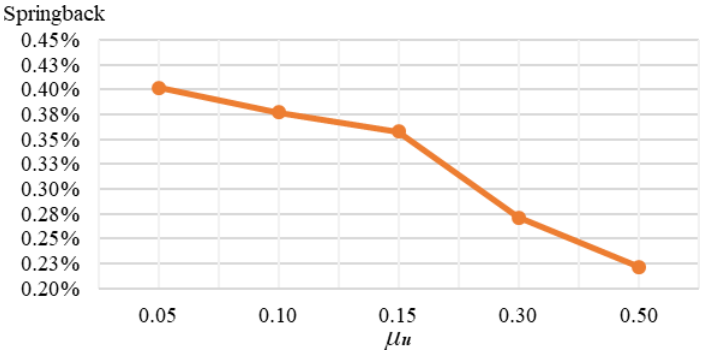

Fig. 10: Upper friction coefficient effect in springback

3.3 Friction coefficient between lower surface and die effect

It is usually preferable the coefficient of friction between the die and the blank to be as low as possible. Even excess lubrication does not raise major concerns on these surfaces, except for cases with complex die shapes or large areas, such as car door stamping, in which excess lubricant can cause deviations during work.

3.3.1 In thickness distribution

Considering the values shown in Table 11, it appears that from μ = 0.3 there is a failure. There is also a trend of displacement of the failure region, which starts in the region '3' to μ = 0.2 and μ = 0.25, moves to '4' when μ = 0.3 and ends in '5 ', in a region corresponding to the side walls of the cup, for μ = 0.4 and μ = 0.5. This trend is even clearly noticed by analyzing Fig. 11.

Table 11: Lower friction coefficient effect in thickness distribution

	Fluid lubricant			Solid lubricant				
Measured Locations (mm)	μ_l							
	0.05	0.1	0.15	0.2	0.25	0.3	0.4	0.5
1	1.245	1.240	1.235	1.230	1.224	1.223	1.217	1.212
2	1.228	1.222	1.216	1.211	1.209	1.210	1.208	1.205
3	1.155	1.134	1.111	1.090	1.092	1.153	1.186	1.190
4	1.171	1.163	1.151	1.136	1.118	1.044	1.129	1.127
5	1.162	1.160	1.157	1.152	1.140	1.106	1.054	1.014
6	1.190	1.188	1.184	1.178	1.165	1.148	1.134	1.128
7	1.188	1.186	1.181	1.174	1.161	1.143	1.130	1.125
8	1.190	1.188	1.185	1.179	1.167	1.151	1.139	1.134
Average	1.191	1.185	1.178	1.169	1.159	1.147	1.150	1.142
						Failure occurred		

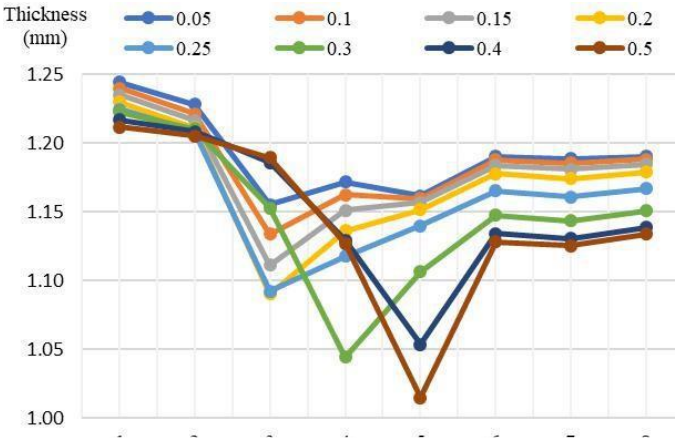

Fig. 11: Lower friction coefficient effect in thickness distribution

3.3.2 In thinning

From the results obtained for the effect of the friction coefficient of the die with the blank, shown in Table 12 and Fig. 12, it is possible to notice, as before, two peaks in the thinning averages, one at μ = 0.3 and the other at μ = 0.5, both with results very close, characterized as the coefficients that result in a worse uniformity of the piece. From another perspective, good uniformity is observed as the friction coefficient decreases, with the μ value range between 0.05 and 0.15 being the most beneficial in relation to the thickness homogeneity.

Table 12: Lower friction coefficient effect in thinning

	Fluid lubricant			Solid lubricant				
Measured Locations (mm)	μ_l							
	0.05	0.1	0.15	0.2	0.25	0.3	0.4	0.5
1	0.037	0.033	0.029	0.025	0.020	0.019	0.014	0.010
2	0.024	0.018	0.014	0.010	0.007	0.009	0.007	0.004
3	0.038	0.055	0.074	0.092	0.090	0.039	0.012	0.009
4	0.024	0.031	0.041	0.053	0.069	0.130	0.059	0.061
5	0.032	0.034	0.036	0.040	0.050	0.078	0.122	0.155
6	0.008	0.010	0.013	0.019	0.029	0.044	0.055	0.060
7	0.010	0.012	0.016	0.021	0.033	0.047	0.058	0.062
8	0.008	0.010	0.013	0.018	0.028	0.041	0.051	0.055
Average	0.022	0.025	0.029	0.035	0.041	0.051	0.047	0.052
%	2.24	2.54	2.95	3.47	4.08	5.09	4.72	5.19

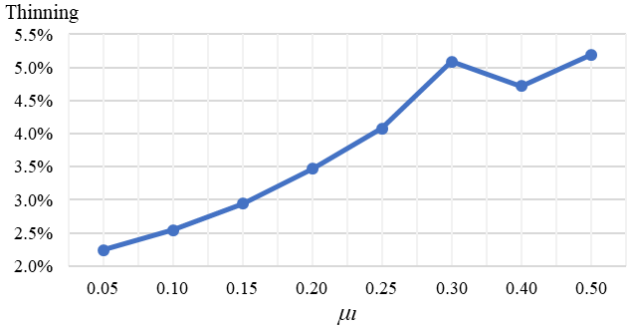

Fig.12: Lower friction coefficient effect in thinning

3.3.3 In springback

Table 13: Lower friction coefficient effect in springback (%)

Fluid lubricant			Solid lubricant		
0.05	0.1	0.15	0.2	0.25	0.3 - 0.5
0.388	0.373	0.358	0.347	0.336	**Failure occurred**

Table 13 and Fig. 13 shows the results obtained for the springback and they proved to be quite similar for the range of μ = 0.5 to μ = 0.25, so this would not be a critical criterion for choosing the coefficient. Summing up, μ values between 0.1 and 0.15 would be preferable due to their good results for blank uniformity and springback.

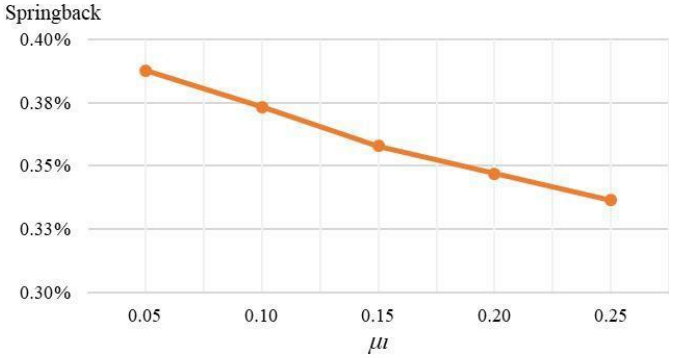

Fig. 13: Lower friction coefficient effect in springback

IV. CONCLUSIONS

The results obtained in the simulations brought important reflections related to the effect of friction and blank holder force on springback behavior, thickness distribution and thinning, consenting with the studied literary references and therefore attesting its validity as a prediction model.

By the results, it is possible to confirm that the region most prone to failure during deep drawing is the bottom edge of the cup, where its fragility is concentrated. It is also possible to notice a displacement of the failure zone in the direction of the edge towards the walls of the cup as the coefficient of friction between the die and the upper surface of the blank increases.

REFERENCES

[1] Sivanandini, M., Dhami, S. S., & Pabla, B. S. (2012). Formability of magnesium alloys. Int. Journal of Modern Engineering Research, 2(4).

[2] Bieler, T. R., Mishra, R. S., & Mukherjee, A. K. (1996). Superplasticity in hard-to-machine materials. Annual Review of Materials Science, 26(1), 75-106. Doi: 10.1146/annurev.ms.26.080196.000451

[3] Experimental and numerical study of warm deep drawing of AZ31 magnesium alloy sheet. International Journal of Machine Tools and Manufacture, 47(3-4), 436-443. doi:https://doi.org/10.1016/j.ijmachtools.2006.06.013

[4] Palaniswamy, H., Ngaile, G., & Altan, T. (2004). Finite element simulation of magnesium alloy sheet forming at elevated temperatures. Journal of Materials Processing Technology, 146(1), 52-60. doi: 10.1016/S0924-0136(03)00844-6

[5] Takuda, H., & Hatta, N. (1998). Numerical analysis of formability of a commercially pure zirconium sheet in some sheet forming processes. Materials Science and Engineering: A, 242(1-2), 15-21. doi: https://doi.org/10.1016/S0921-5093(97)00520-0

[6] Simulia, D. (2011). ABAQUS 6.11 analysis user's manual. Abaqus, 6, 22-2.

[7] Mathaudhu, S. N., & Nyberg, E. A. (2016). Magnesium alloys in US military applications: past, current and future solutions. In Essential readings in magnesium technology (pp. 71-76). Springer, Cham.

[8] Cheng, Y. Q., Zhang, H., Chen, Z. H., & Xian, K. F. (2008). Flow stress equation of AZ31 magnesium alloy sheet during warm tensile deformation. Journal of materials processing technology, 208(1-3), 29-34. doi: https://doi.org/10.1016/j.jmatprotec.2007.12.095

[9] Reddy, A. C. S., Rajesham, S., & Reddy, P. R. (2015). Experimental and simulation study on the warm deep drawing of AZ31 alloy. Advances in Production Engineering & Management, 10(3), 153. doi: http://dx.doi.org/10.14743/apem2015.3.199

[10] David, S., Jeff, L., & John, G. (2003). Fundamentals of tool design. American society of tool and manufacturing engineers.

[11] Lazarescu, L., Nicodim, I., & Banabic, D. (2015). Evaluation of drawing force and thickness distribution in the deep-drawing process with variable blank-holding. In Key Engineering Materials (Vol. 639, pp. 33-40). Trans Tech Publications Ltd. doi: 10.4028/www.scientific.net/KEM.639.33

[12] Soualem, A. (2013). A Detailed Experimental Study of the Springback Anisotropy of Three Metals using the Stretching-Bending Process. International Journal of Mechanical and Mechatronics Engineering, 7(1), 144-147. doi: doi.org/10.5281/zenodo.1083833

[13] Mang, T., & Dresel, W. (Eds.). (2007). Lubricants and lubrication. John Wiley & Sons.